Short communication

Stepwise construction and destruction of nickel thiolate Ni_3 cluster revealed by mass spectrometry and crystallography

Min Tu[a], Jie Wang[b], Bin Liu[a,*], Ming-Hua Zeng[a,b,*]

[a] *Hubei Collaborative Innovation Center for Advanced Organic Chemical Materials, Ministry of Education Key Laboratory for the Synthesis and Application of Organic Functional Molecules, College of Chemistry and Chemical Engineering, Hubei University, Wuhan 430062, PR China*
[b] *Department Key Laboratory for the Chemistry and Molecular Engineering of Medicinal Resources, School of Chemistry and Pharmaceutical Sciences, Guangxi Normal University, Guilin 541004, PR China*

GRAPHICAL ABSTRACT

A nickel thiolate cluster $[Ni_3L_3S]NO_3$ (HL = (1-methyl-1H-benzo[d]imidazol-2-yl)methanethiol) was synthesized and its formation process was studied by mass spectrometry.
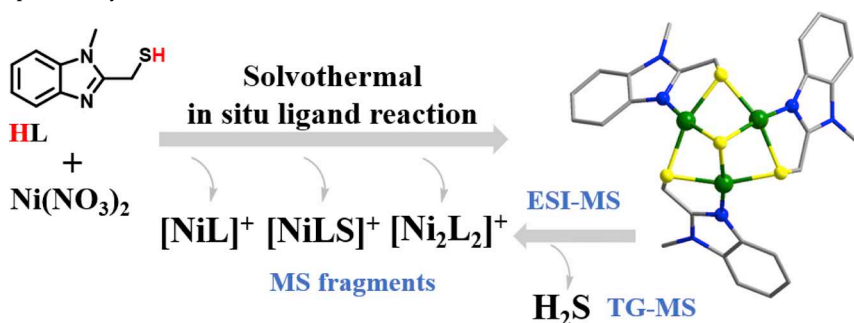
ARTICLE INFO

ABSTRACT

Trinuclear nickel thiolate cluster $[Ni_3(\mu_3\text{-}S)(L)_3]NO_3$ (HL = (1-methyl-1H-benzo[d]imidazol-2-yl)methanethiol) (**1**) has been synthesized from $Ni(NO_3)_2 \cdot 6H_2O$ and HL at solvothermal condition at 80 °C using methanol as solvent. It has been characterized by X-ray single crystal diffraction, elemental analysis, electrospray ionization mass spectrometry (ESI-MS), and thermogravimetric analysis. The stability of the cluster in methanol is reflected by the fact that the molecular ion peak of $[Ni_3(\mu_3\text{-}S)(mbms)_3]^+$ is dominant in ESI-MS. Furthermore, the release of H_2S from **1** was observed at elevated in source energy condition and in tandem mass spectrometry. The H_2S fragment was also detected during the destruction of **1** by thermogravimetric analysis combined with mass spectrometry (TG-MS). Key fragments $[NiLS]^+$ and $[Ni_2L_2]^+$ were perceived in solution by ESI-MS during the reaction, which have also been detected at elevated in source energy condition. A plausible stepwise assembly process including $[NiL]^+$ to the mixture of $[NiLS]^+$ and $[Ni_2L_2]^+$ which then combined to give the product $[Ni_3L_3S]^+$ was proposed.

* Corresponding author at: Hubei Collaborative Innovation Center for Advanced Organic Chemical Materials, Ministry of Education Key Laboratory for the Synthesis and Application of Organic Functional Molecules, College of Chemistry and Chemical Engineering, Hubei University, Wuhan 430062, PR China.
 E-mail addresses: liubin@hubu.edu.cn (B. Liu), zmh@mailbox.gxnu.edu.cn (M.-H. Zeng).

1. Introduction

One of the primary goals in chemistry is to disclose the reaction bonding pathway so that the mechanisms can be drawn [1–5]. As model complex for many enzymes, transition metal thiolates have been attracting much research interest [6]. Among them, the research of the chemistry of Ni_3S_4 trinuclear sulfide thiolate clusters [7–9] is important due to the unique biological function of Ni−S sites as in hydrogenase. Understanding the reaction pathway of the formation of Ni_3S_4 cluster is not only vital for the development of new nickel thiolate clusters but also important for the exploration of the chemistry of the hydrogenase. However, the formation process has not been revealed in detail. This could hinder the design and synthesis of new nickel thiolate clusters with hydrogenase activities.

Electrospray ionization mass spectrometry (ESI-MS) is a powerful technique to give instant information of intermediate species not only in organic reactions but also the assembly of the complicated transition metal containing coordination clusters [1,10]. Our group has also made some contributions in this area and the combination of ESI-MS and X-ray crystallography technique has been successfully applied on the elucidation of the assembly processes of Co4 [11], Zn14 [12], Fe3 [13], Zn5 [14], and Ni7 + 1 [15]. As a continuation of the work on assembly process study, in this paper, a new Ni_3S_4 cluster $[Ni_3(\mu_3\text{-}S)L_3]NO_3$ (**1**) (HL = (1-methyl-1H-benzo[*d*]imidazol-2-yl)methanethiol) has been readily synthesized from the reaction of HL and $Ni(NO_3)_2\cdot 6H_2O$ in solvothermal conditions at 80 °C. Its construction and destruction process has been revealed through ESI-MS, tandem mass spectrometry, and thermogravimetric analysis combined with mass spectrometry (TG-MS). It is worth noting that, for the first time, releasing of H_2S from Ni_3S_4 cluster is observed in ESI-MS and H_2S was further detected by TG-MS.

2. Results and discussion

2.1. Crystal structure of [Ni₃(μ₃-S)L₃]NO₃

At solvothermal condition, $Ni(NO_3)_2\cdot 6H_2O$ reacts with (1-Methyl-1H-benzo[*d*]imidazol-2-yl)methanethiol (HL) in methanol at 80 °C for 24 h to produce black crystals which is characterized as compound **1**. As shown in Fig. 1, compound **1** crystallizes in the trigonal *P*-3*c*1 space group and consists of three Ni atoms, three L ligands, three μ_2-S atoms, one μ_3-S atom, and one NO_3^- counterion (Table S1). The oxidation state of the three Ni atoms are ascribed to + 2, by considering the charge-balance, bond valence sum calculation, and the existence of classical bond lengths for Ni^{II} (Table S2). The coordination sphere around each Ni is a distorted square-planar, which is suggested by

calculation of the continuous-shape measurement value (Table S3). Each Ni^{II} ion is coordinated by 1 L ligand through N1 and μ_2-S (S1) atom, one μ_2-S atom S1′ from another L ligand, and one apical μ_3-S atom (S2). The source of the apical S atom might come from in-situ ligand reaction of thiol ligand L at solvothermal condition [16]. The bond angles of N1-Ni1-S2 (171.0°) and S1-Ni1-S1′ (161.9°) also reflected this coordination mode. The bond lengths of Ni-(μ_3-S) (2.1792(12) Å to 2.1801(112) Å), Ni-(μ_2-S) (2.1890(9) Å to 2.2050(14) Å), and Ni−N (1.899(3) Å) are comparable to those of $[Ni_3(\mu_3\text{-}S)(bms)_3]NO_3\cdot C_2H_5OH$ (Hbms = (1H-benzoimidazol2-yl)-methanethiol) [8]. An equilateral triangle is formed by the three Ni atoms, and the distance between Ni1 and Ni1′ are 2.767 Å which are shorter than that of $[Ni_3(\mu_3\text{-}S)(bms)_3]$ $NO_3\cdot C_2H_5OH$ [8]. The Ni^{II} ions are bridged by μ_2-S atoms to each other (Ni1-S1-Ni1′ = 78.03(4)°) and these six atoms are almost coplanar with the maximum deviation from the mean plane is −0.012 Å for Ni1 and 0.012 Å for S1, respectively. This Ni_3S_3 plane is capped by the μ_3-S atom on one side and three ligands L on the other, making a cone shaped molecule with the μ_3-S atom at the apex. The bond lengths of Ni−S and Ni−N and bond angles around Ni and S atoms are among the range of the reported cone shaped Ni_3S_4 clusters (Table S2). The NO_3^- ion is bound into the cavity through a benzylic C−H hydrogen bond (C8-H8···O1, 2.324 Å, Fig. S2a, Table S4). Furthermore, the O atom of the NO_3^- ion is also hydrogen bonded to a C−H (C5-H5···O1, 2.420 Å; C9-H9B···O1, 2.56 Å) of another molecule (Fig. S2b). The weak interaction of C-H···S hydrogen bond also exists between adjacent molecules with H···S distance of 2.932 Å and C8-H8A···S1 angle of 115° (Fig. S2c). Hirshfeld surface analysis has also been used to explore the weak interaction (Table S5, S6). It is found that the weak interaction of **1** is comparable with the $[Ni_3(\mu_3\text{-}S)(bms)_3]NO_3\cdot C_2H_5OH$ [8], showing that the substituent in N atom of the benzimidazole has little influence for the intermolecular interaction. In addition, the reaction condition to produce compound **1** (80 °C, 24 h) is much milder than that for $[Ni_3(\mu_3\text{-}S)(bms)_3]NO_3\cdot C_2H_5OH$ (140 °C, 3 days).

2.2. ESI-MS of [Ni₃(μ₃-S)L₃]NO₃

While a series of $[Ni_3S_4]$ clusters containing μ_3-S atom as apex have been reported (Table S2), their formation process has not been reported. ESI-MS, as a powerful method to percept transient intermediates in complicated reactions, has been applied widely on the mechanism study in both organic and coordination chemistry [1]. Therefore, the reaction process of the formation of $[Ni_3(\mu_3\text{-}S)L_3]NO_3$ has been studied through ESI-MS. First, the ESI-MS of the crystal was recorded for a reference. As shown in Fig. 2a, when the in-source energy is 0 eV, the main fragment $[Ni_3(\mu_3\text{-}S)L_3]^+$ (m/z 738.92, Fig. 2b, Table S7) is ascribed to the molecular ion peak of $[Ni_3(\mu_3\text{-}S)L_3]NO_3$,
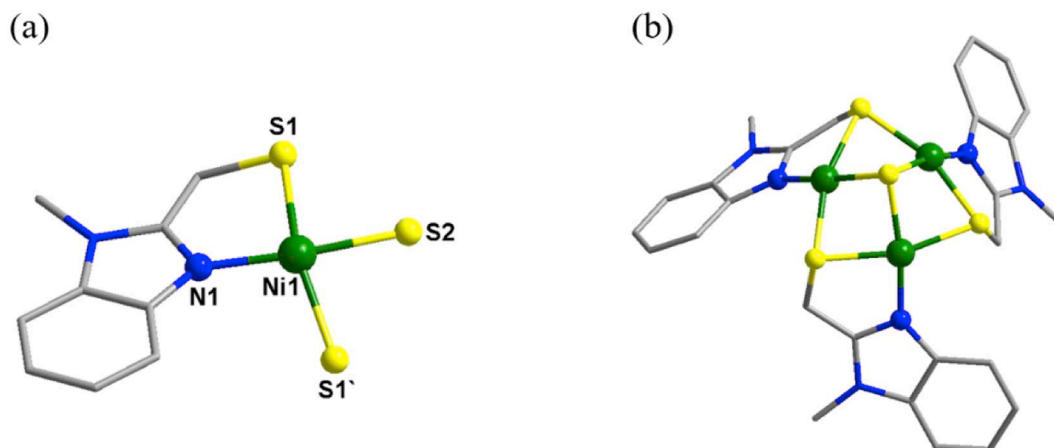
Fig. 1. (a) Coordination mode of Ni cation in compound **1**, (b) Crystal structure of compound **1**. (Color scheme: Ni, green; S, yellow; N, blue; C, gray. Hydrogen atoms and counter ion are omitted for clarity). (For interpretation of the references to color in this figure legend, the reader is referred to the web version of this article.)
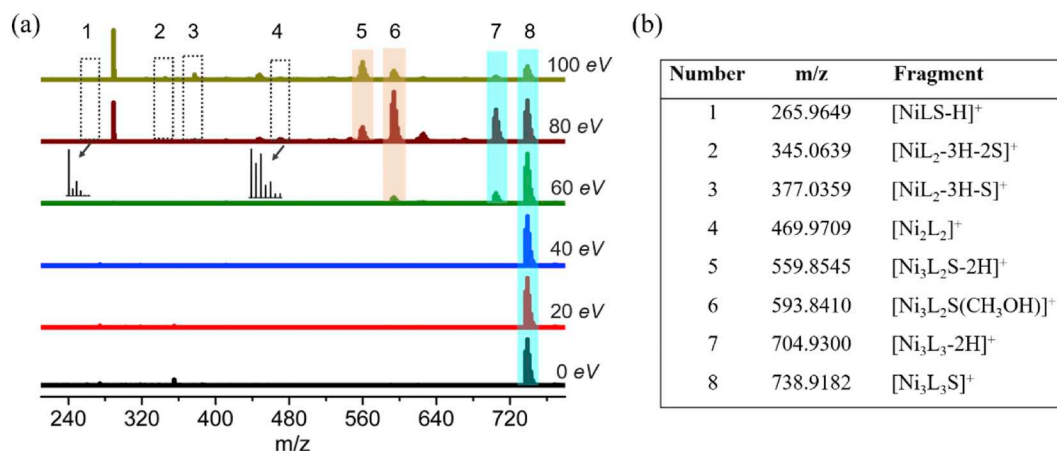
Fig. 2. (a) Positive-mode ESI-MS spectra of dissolved crystals of **1** for different in source energies, (b) assignment of major species.

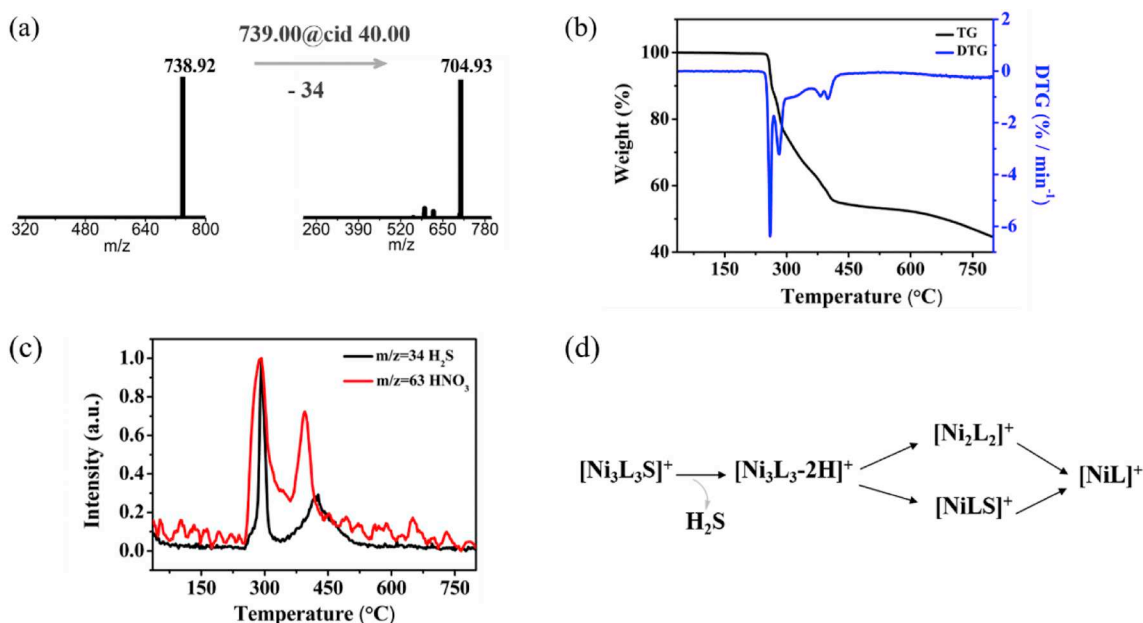| Number	m/z	Fragment
1	265.9649	$[NiLS-H]^+$
2	345.0639	$[NiL_2-3H-2S]^+$
3	377.0359	$[NiL_2-3H-S]^+$
4	469.9709	$[Ni_2L_2]^+$
5	559.8545	$[Ni_3L_2S-2H]^+$
6	593.8410	$[Ni_3L_2S(CH_3OH)]^+$
7	704.9300	$[Ni_3L_3-2H]^+$
8	738.9182	$[Ni_3L_3S]^+$

Fig. 3. (a) Tandem mass spectrometry of **1** (738.92 as "parent" ion), (b) Thermogravimetric Analysis-Differential Thermal Gravity (TG-DTG) curves of compound **1**, (c)Thermogravimetric Analysis Combined with Mass Spectrometry (TG-MS) of compound **1**, and (d) possible destruction pathway.

which suggests that the product is stable in methanol. The destructive processes of $[Ni_3(\mu_3\text{-}S)L_3]NO_3$ monitored by ESI-MS at variable in-source energies were also carried out to get more information. It is worth noting that at 20 eV and 40 eV, no appreciable fragments were detected, further indicating the high stability of the product. At 60 eV, two new fragments peaks $[Ni_3L_3-2H]^+$ (m/z 704.93) and $[Ni_3L_2S(CH_3OH)]^+$ (m/z 593.84) were observed. At 80 eV, fragments $[Ni_3L_2S-2H]^+$ (m/z 559.85), $[Ni_2L_2]^+$ (m/z 469.97), $[NiL_2-3H-S]^+$ (m/z 377.04), $[NiL_2-3H-2S]^+$ (m/z 345.06), and $[NiLS]^+$ (m/z 265.96) were observed, suggesting the further decomposition. These fragments might be helpful to elucidate the assembly process of compound **1**. In addition, we speculated that the formation of fragment $[Ni_3L_3-2H]^+$ might come from the extrusion of H_2S from $[Ni_3L_3S]^+$. This phenomenon was also observed in the tandem mass spectrometry (Fig. 3a). When the peak at 738.92 ($[Ni_3(\mu_3\text{-}S)L_3]^+$) was selected as "parent" ion, the exclusive "daughter" ion is found at 704.93 ($[Ni_3L_3-2H]^+$), indicating the loss of a fragment with m/z 34. Thermogravimetric analysis (TGA, Fig. 3b) also reveals that **1** undergoes weight loss of 11.5% from 242 °C to 270 °C, corresponding to the departure of one H_2S and one HNO_3 (calcd. 12%). Then TG-MS (Fig. 3c) was applied and the peak at m/z 34 assigning to H_2S was detected, further confirming that **1** could produce

H_2S by decomposition. While the extrusion of SO_2 from nickel thiolates have been reported [17], to our knowledge, this is the first time that the formation of H_2S from the decomposition of nickel thiolate was observed. A plausible stepwise destruction pathway was proposed in Fig. 3d.

2.3. Reaction process study

Time-dependent ESI-MS was applied to monitor the species of the formation of **1**. As shown in Fig. 4, after the starting materials were mixed together, fragment $[NiL(H_2O)Na]^+$ (m/z 275.96, Fig. S5, Table S8) was observed, suggesting the coordination of ligand L and Ni^{2+}. Furthermore, the fragments $[NiLS(H_2O)Na]^+$ (m/z 307.97), $[NiLS(H_2O)_2Na]^+$ (m/z 326.97), and $[NiLSH_2NaNO_3]^+$ (m/z 353.95) were also percepted and the S atom in them might come from ligand L through C−S bond cleavage [8,18,19]. Although the detailed mechanism of the formation of S is not clear yet, the assembly of fragment $[NiL(H_2O)Na]^+$ with S atom could afford the fragments $[NiLS(H_2O)Na]^+$ and $[NiLS(H_2O)_2Na]^+$, respectively. At 0.5 h, $[Ni_2L_2Na(CH_3OH)_3]^+$ (m/z 589.08) was percepted, which might come from fragment $[NiL(H_2O)Na]^+$. At 1 h, the fragment $[Ni_3L_3S]^+$
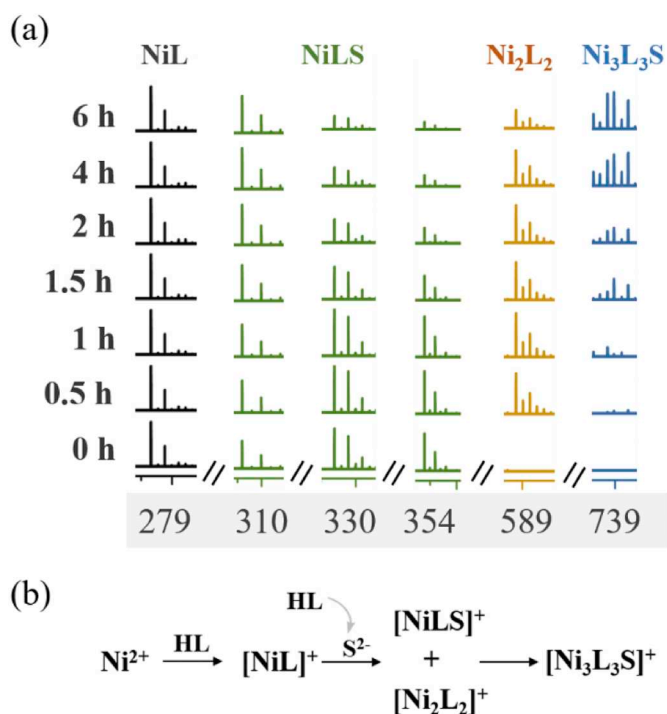
Fig. 4. (a) Selected fragments in time-dependent ESI-MS spectra of the reaction solution (positive mode) and (b) possible stepwise assembly process to produce compound **1**.

corresponding to the product was observed, which might come from the assembly of $[NiLS]^+$ and $[Ni_2L_2Na(CH_3OH)_3]^+$. It is worth noting that the fragments $[NiL]^+$, $[NiLS]^+$, $[Ni_2L_2]^+$ were observed from the ESI-MS spectra of the product at elevated in source energy (80 eV). Based on these results, a plausible mechanism for the formation of compound **1** was proposed (Fig. 4b). First, the coordination of Ni^{2+} with ligand HL through deprotonation could afford $[NiL]^+$, then the cleavage of C−S bond in L could give S atom which coordinates with $[NiL]^+$ to give $[NiLS]^+$. In the meanwhile, the assembly of $[NiL]^+$ might afford $[Ni_2L_2]^+$ which could combine with $[NiLS]^+$ to produce the $[Ni_3L_3S]^+$ fragment.

In summary, a new nickel sulfide thiolate cluster $[[Ni_3(\mu_3\text{-}S)L_3]NO_3$ has been successfully synthesized from $Ni(NO_3)_2·6H_2O$ and HL at solvothermal condition with relatively lower temperature and shorter time. The reaction process has been monitored by ESI-MS. A plausible mechanism involving stepwise assembly ($[NiL]^+$ to $[NiLS]^+$ and $[Ni_2L_2]^+$ and finally $[Ni_3L_3S]^+$) was proposed based on these results together with the destructive processes at variable in-source energies. It is worth noting that, for the first time, the release of H_2S at elevated in-source energies was observed from ESI-MS spectra and further confirmed by tandem mass spectrometry and TG-MS. These results show that the combination of multiple MS techniques such as time-dependent ESI-MS, tandem mass spectrometry, and TG-MS with X-ray crystallography could be used to study the formation and destruction processes of the nickel thiolate cluster, which is helpful for the understanding and designing new transition metal thiolate clusters with active M-S sites as in hydrogenase.

Appendix A. Supplementary material

Supplementary data to this article can be found online at https://doi.org/10.1016/j.inoche.2019.05.014.

References

[1] D. Schröder, Applications of electrospray ionization mass spectrometry in mechanistic studies and catalysis research, Acc. Chem. Res. 45 (2012) 1521–1532.

[2] S. Datta, M.L. Saha, P.J. Stang, Hierarchical assemblies of supramolecular coordination complexes, Acc. Chem. Res. 51 (2018) 2047–2063.

[3] D.J. Tranchemontagne, J.L. Mendoza-Cortés, M. O'Keeffe, O.M. Yaghi, Secondary building units, nets and bonding in the chemistry of metal–organic frameworks, Chem. Soc. Rev. 38 (2009) 1257–1283.

[4] T.G. Saint-Denis, R.Y. Zhu, G. Chen, Q.F. Wu, J.Q. Yu, Enantioselective C(sp(3))H bond activation by chiral transition metal catalysts, Science 359 (2018) eaao4798.

[5] Q.-F. Sun, S. Sato, M. Fujita, An M18L24 stellated cuboctahedron through post-stellation of an M12L24 core, Nat. Chem. 4 (2012) 330–333.

[6] E. Bouwman, J. Reedijk, Structural and functional models related to the nickel hydrogenases, Coord. Chem. Rev. 249 (2005) 1555–1581.

[7] S.D. Han, X.H. Miao, S.J. Liu, X.H. Bu, A series of cobalt and nickel clusters based on thiol-containing ligands accompanied by in situ ligand formation, Dalton Trans. 44 (2015) 560–567.

[8] J.J. Guo, W. Wang, Y.D. Zhang, L. Yang, S.H. Zhang, X.Q. Zhang, Solvothermal syntheses and structures of three clusters based on (1H-benzoimidazol-2-yl)-methanethiol, J. Coord. Chem. 66 (2013) 1467–1476.

[9] H. López-Sandoval, A. Richaud, R. Contreras, G. Jeffery Leigh, P.B. Hitchcock, A. Flores-Parra, J. Carlos Galvez-Ruíz, A. Cruz, H. Nöth, N. Barba-Behrens, Triangulo-μ3-sulfido-trinickel(II) cone-shaped clusters and anion traps: structural characterization, Polyhedron 23 (2004) 1837–1843.

[10] K.L. Vikse, Z. Ahmadi, J. Scott McIndoe, The application of electrospray ionization mass spectrometry to homogeneous catalysis, Coord. Chem. Rev. 279 (2014) 96–114.

[11] H.-L. Zheng, X.-L. Chen, T. Li, Z. Yin, Y. Zhang, M. Kurmoo, M.-H. Zeng, Manipulating clusters by use of competing N,O-chelating ligands: a combined crystallographic, mass spectrometric, and DFT study, Chem. Eur. J. 24 (2018) 7906–7912.

[12] X.-L. Chen, H.-B. Xu, X.-X. Shi, Y. Zhang, T. Yang, M. Kurmoo, M.-H. Zeng, Hierarchical assembly and aggregation-induced enhanced emission of a pair of isostructural Zn14 clusters, Inorg. Chem. 56 (2017) 14069–14076.

[13] J.-P. Zhong, B. Liu, T. Yang, Y.-J. Liu, Z.-H. Zhu, B.-F. Shi, M. Kurmoo, M.-H. Zeng, Tracking the progress and mechanism study of a solvothermal in situ domino N-alkylation reaction of triethylamine and ammonia assisted by ferrous sulfate, Inorg. Chem. 56 (2017) 10123–10126.

[14] M.-H. Zeng, Z. Yin, Z.-H. Liu, H.-B. Xu, Y.-C. Feng, Y.-Q. Hu, L.-X. Chang, Y.-X. Zhang, J. Huang, M. Kurmoo, Assembly of a highly stable luminescent Zn5 cluster and application to bio-imaging, Angew. Chem. Int. Ed. 55 (2016) 11407–11411.

[15] H.-X. Na, P.-Y. Yang, Z. Yin, Y.-H. Wang, L.-X. Chang, R. Si, M. Kurmoo, M.-H. Zeng, Stepwise assembly of MII7 clusters revealed by mass spectrometry, EXAFS, and crystallography, Chem. Eur. J. 22 (2016) 18404–18411.

[16] X.-M. Chen, M.-L. Tong, Solvothermal in situ metal/ligand reactions: a new bridge between coordination chemistry and organic synthetic chemistry, Acc. Chem. Res. 40 (2007) 162–170.

[17] R.M. Buonomo, I. Font, M.J. Maguire, J.H. Reibenspies, T. Tuntulani, M.Y. Darensbourg, Study of sulfinate and sulfenate complexes derived from the oxygenation of thiolate sulfur in [1,5-Bis(2-mercapto-2-methylpropyl)-1,5-diazacyclooctanato(2-)]nickel(II), J. Am. Chem. Soc. 117 (1995) 963–973.

[18] Z.-M. Hao, R.-Q. Fang, H.-S. Wu, X.-M. Zhang, Cu6S4 cluster based twelve-connected face-centered cubic and Cu19I4S12 cluster based fourteen-connected body-centered cubic topological coordination polymers, Inorg. Chem. 47 (2008) 8197–8203.

[19] Y.-K. He, Z.-B. Han, Y. Ma, X.-D. Zhang, Syntheses, crystal structures and luminescence properties of lanthanide coordination polymers involving in situ C–S bond cleavage of (4-pyridylthio)acetic acid, Inorg. Chem. Commun. 10 (2007) 829–832.